Full Wave Optimization of Stripline Tapped-in Ridge Waveguide Bandpass Filters

Mahmoud A. El Sabbagh †, Heng-Tung Hsu †, Kawthar A. Zaki †, Protap Pramanick ‡ and Tim Dolan ‡

†Electrical and Computer Engineering department, University of Maryland, College Park, MD 20742

‡ K & L Microwave Incorporated, Salisbury, MD 21801

Abstract— **A bandpass ridge waveguide filter, with input/output realized through tapped-in stripline is designed. Using rigorous mode matching technique the generalized scattering matrices of all the building blocks can be obtained. Design procedure is described and examples are given to demonstrate the features of the proposed coupling structure. The proposed structure shows a considerable reduction of the filter's total length.**

I. INTRODUCTION

In modern communication systems, there is a growing need for small size, light weight and compact high performance RF/microwave elements. Since large areas in the printed circuit boards of systems are usually occupied by passive components, integration of the passive components into multilayers substrates [1] is an efficient way to miniaturize the size and to increase the reliability of the RF/microwave systems. RF and microwave filters are very important passive components, among which, 3-D cavity filters usually offer lower loss characteristics compared to the planar circuits [2]. A typical filter to meet these requirements is the ridge waveguide filter as it is characterized by large single mode broadband operation, the dominant mode cutoff frequency of the ridge waveguide is smaller than that of a rectangular waveguide with the same cross section, low loss, high spurious performance and compact size. Ridge waveguide filter designs suitable for multilayers applications can be found in [3], [4] and [5]. Fig. 1(a) [5] shows the configuration of a typical ridge waveguide filter that consists of single ridge waveguide resonators. The coupling between each two resonators is achieved through a section of rectangular waveguide, with evanescent mode, operating below the cutoff frequency of the dominant mode of the single ridge waveguide. This typical configuration of ridge waveguide filters makes them useful in designing compact filters that have moderate to wide bandwidth operation and good spurious performance. Transitions from the single ridge waveguide at the input and the output to the stripline as shown in Fig. 1(b) [4] is designed to make the filter compatible with other components in multilayers packages. Very good results were obtained for filters designed according to the configuration in Fig. 1. However, the problem is that going from the input/output ridge waveguides to the 50Ω stripline involves a long transition (multisections of striplines), redundant input/output ridges and evanescent sections at the input and the output for coupling realization thus increasing the filter's total length. It is proposed in this paper to replace the input and output transformer couplings by direct tapped connections to the first and the last resonators as shown in Fig. 2(a). In the examples included in this paper, the resulting total filter's length reduction is between 36% and 70%. The full wave mode matching technique is used to obtain the generalized scattering matrices of all the building blocks. The building blocks are cascaded together to get the total filter's response. Full wave optimization is used to get the optimum filter's response.

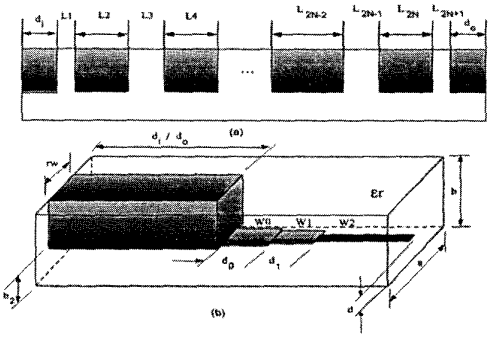

Fig. 1. (a) Configuration of a N poles ridge waveguide filter. (b) Transition from single ridge waveguide to 50Ω stripline at the input and the output. Dimensions: $N = 5$, $a = 0.3''$, $b = 0.096''$, $b_2 = 0.012''$, $d = 0.012''$, $rw = 0.1''$, $\epsilon_r = 3.38$, $d_i = d_o = 0.030''$, $L_1 = 0.0837''$, $L_2 = 0.1239''$, $L_3 = 0.2123''$, $L_4 = 0.0968''$, $L_5 = 0.2576''$, $L_6 = 0.0949''$, $L_7 = L_5$, $L_8 = L_4$, $L_9 = L_3$, $L_{10} = L_2$, $L_{11} = L_1$, stripline thickness= $0.0005''$, $W_0 = 0.060''$, $W_1 = 0.030''$, $W_2 = 0.0215''$, $d_0 = 0.115''$, $d_1 = 0.145''$

II. MODELING AND DESIGN

The proposed filter's structure shown in Fig. 2(a) is decomposed into building blocks characterized by their

0-7803-7239-5/02/$10.00 © 2002 IEEE

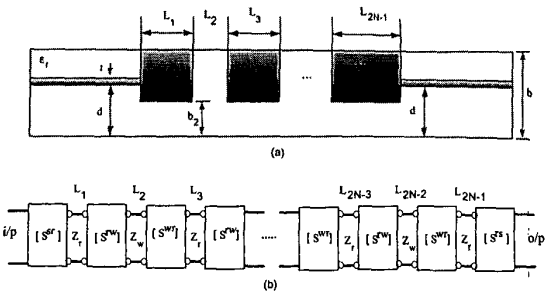

Fig. 2. (a) Configuration of a N poles ridge waveguide filter excited by a tapped-in 50Ω stripline. Dimensions: $N = 5$, $a = 0.3''$, $b = 0.096''$, $b_2 = 0.012''$, $d = 0.044''$, $rw = 0.1''$, $\epsilon_r = 3.38$, $t = 0.0005''$, $L_1 = 0.1084''$, $L_2 = 0.2027''$, $L_3 = 0.0968''$, $L_4 = 0.252''$, $L_5 = 0.0953''$, $L_6 = L_4$, $L_7 = L_3$, $L_8 = L_2$, $L_9 = L_1$, $W_0 = 0.0545''$. (b) Generalized scattering matrices building blocks.

generalized scattering matrices. The building blocks as shown in Fig. 2(b) are the discontinuity from the stripline to the single ridge waveguide $[S^{sr}]$, the discontinuity from the ridge waveguide to the rectangular waveguide $[S^{rw}]$ and $[S^{wr}]$ is the discontinuity from the rectangular waveguide to the ridge waveguide. The generalized scattering matrices of these building blocks are obtained using the full wave mode matching technique. Before applying the mode matching, the eigenmodes in the stripline and in the ridge waveguide are to be found first.

A. Eigenmodes

The modes in the stripline can be classified into TEM, TE and TM modes. While, the modes in the ridge waveguide can be classified into TE and TM modes. For each of these modes, eigenfields within the guides are to be found first. The approach of getting the eigenmodes and their field distributions can be found in [2].

B. Generalized Scattering Matrix

After obtaining the eigenmodes and the corresponding field components, the mode matching technique is applied to obtain the generalized scattering matrices of all the discontinuities involved. At each side of a discontinuity, the fields are expressed as the superposition of the incident and the reflected waves of all the eigenmodes that are orthogonal and constitute a complete set of basis functions. By applying the boundary conditions at each discontinuity and performing appropriate inner products of these eigenmode fields, the generalized scattering matrices of the discontinuities are obtained.

C. Filter Design

Dimensions of the evanescent mode waveguide are determined so that its fundamental mode cutoff frequency is much higher than the filter operating center frequency. The ridge waveguides are chosen to have the same cutoff frequencies. The filter design consists of two steps. The first is the prototype synthesis to get the required impedance inverters [7], [8] for the inner sections of the filter and to realize the required input/output coupling. A modification factor [4] is introduced to modify the fractional bandwidth that turns out to be wider than the desired one due to dispersion and large bandwidth that were not considered in [7]. Fig. 3 shows the configuration and the corresponding building blocks used to compute the input/output coupling. The actual coupling is obtained by using the following equation:

$$R = -\frac{4}{f_l \frac{d\phi}{df}|_{max}} \tag{1}$$

where ϕ is the phase angle of the input reflection coefficient obtained at the reference plane $t - t$, f_l is the loaded resonant frequency that corresponds to the maximum phase angle variation [9]. The stripline dimensions are changed until the required coupling is achieved. The second step is the full wave optimization to get the optimum filter parameters. An objective function [6], [8] is defined and is minimized efficiently using a gradient optimization method together with a numerical interpolation technique.

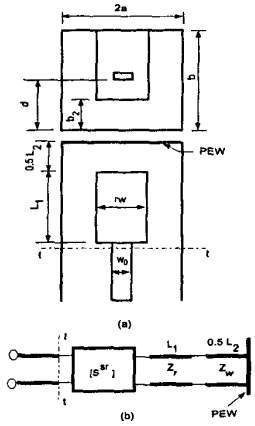

Fig. 3. (a) The configuration used to compute the input/output coupling of a ridge waveguide filter excited by a tapped-in 50Ω stripline. (b) Generalized scattering matrices building blocks.

III. NUMERICAL RESULTS

Two 5 poles ridge waveguide bandpass filters, to have a 6.175 GHz operating center frequency and 0.5 GHz bandwidth, were designed by using the configurations shown in Figs 1, 2. Fig. 4 shows a comparison of the in-band and the out-of-band frequency response of the filter, with input/output transitions, which has a total length of 2223.5 mils and the tapped-in filter which has a total length of 1415.1 mils. The tapped-in filter has a 36.5% reduced length from the conventional filter while it has better return loss in the passband, the conventional filter has better stopband performance. Another interesting application on the same topic is the interdigital bandpass filters. From the analysis point of view, interdigital filters can be modeled exactly the same way as double-ridge waveguide filters. This concept can be well illustrated in Fig. 5, where the cross sections (transverse to the direction of propagation) of the interdigital filters are related to that of double-ridge waveguide filters. To demonstrate the feasibility of this concept, an 8-pole interdigital filter with center frequency 2.14 GHz and 152 MHz bandwidth is designed and manufactured. The detailed dimensions are shown in Fig. 6. The simulated response using rigorous mode matching technique is included in Fig. 7. Fig. 8 shows the experimental results which is in good agreement with the simulated response.

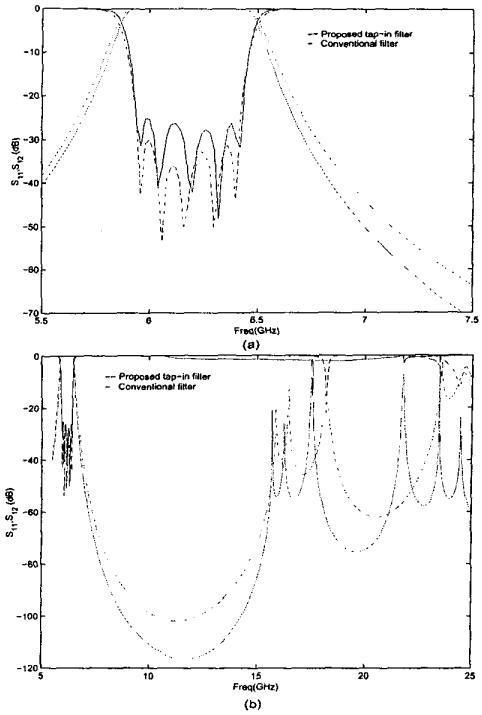

Fig. 4. Comparison of frequency response of the filters shown in Figs. 1, 2 (a) In-band (b) Out-of-band.

IV. CONCLUSION

A bandpass ridge waveguide filter with 50Ω tapped-in stripline is proposed for multilayers compact package. The mode matching technique is used to get the generalized scattering matrices of all the building blocks of the tapped-in ridge waveguide filter. Full wave optimization follows to get the optimum filter parameters. It is shown through designed filters that the tapped-in ridge waveguide filter results in a significant length reduction compared to the conventional filter with input/output transitions and also the filter has a good spurious performance. The accuracy of the numerical results are checked by comparison with HFSS and experimental data are shown.

REFERENCES

[1] A. Bailey, W. Foley, M. Hageman, C. Murray, A. Piloto, K. Sparks, and K. Zaki, "Miniature LTCC filters for digital receivers", *1997 IEEE MTT-S Int. Microwave Symp. Digest*, pp. 999-1002.

[2] C. Wang, "Modeling of Conductor, Dielectric Loaded Resonators, Filters and Double Ridge Waveguide T-Junctions", *Ph.D dissertation 1997*, Electrical and Computer Engineering Department, University of Maryland College Park.

[3] J. Gipprich, D. Stevens, M. Hageman, A. Piloto, K. Zaki, and Y. Rong, "Embedded waveguide filters for microwave and wireless applications using cofired ceramic technologies" *Proc. Int. Microelectron.Symp*, San Diego, CA, Nov. 1998, pp.23-26.

[4] Y. Rong, K. Zaki, M. Hageman, D. Stevens, and J. Gipprich, "Low temperature cofired ceramic (LTCC) ridge waveguide bandpass filters", *1999 IEEE MTT-S Int. Microwave Symp. Digest*, pp. 1147-1150.

[5] Yu Rong, Kawthar Zaki, John Gipprich, Michael Hageman, and Daniel Stevens, "LTCC Wide-band Ridge-Waveguide Bandpass Filters", *IEEE Trans. Microwave Theory Tech.*, vol. MTT-47, No. 9 pp. 1836-1840, Sept. 1999.

[6] Yu Rong, "Modeling of Combline Coaxial, Ridge Waveguide Filers & Multiplexers. *Ph.D dissertation 1999*, Electrical and Computer Engineering Department, University of Maryland College Park.

[7] G. Matthaei, L. Young and E. M. T. Jones, *Microwave Filters, Impedance-Matching Networks, and Coupling Structures*, Norwood, MA: Artech House, 1980.

[8] H. W. Yao, A. E. Abdelmonem, J. F. Liang, X. P. Liang and K. A. Zaki, "Wide-Band Waveguide and Ridge Waveguide T-Junctions for Diplexer Applications", *IEEE Trans. Microwave Theory Tech.*, vol. MTT-41, No. 12, pp. 2166-2173, Dec. 1993.

[9] C. Wang and K. A. Zaki "Modeling of Couplings Between Double-Ridge Waveguide and Dielectric-Loaded Resonator", *IEEE Trans. Microwave Theory Tech.*, vol. MTT-46, No. 12, pp. 2404-2411, Dec. 1998.

[10] Agilent EEsof EDA, Palo Alto, CA "Agilent High Frequency Structure Simulator 5.5", December 1999.

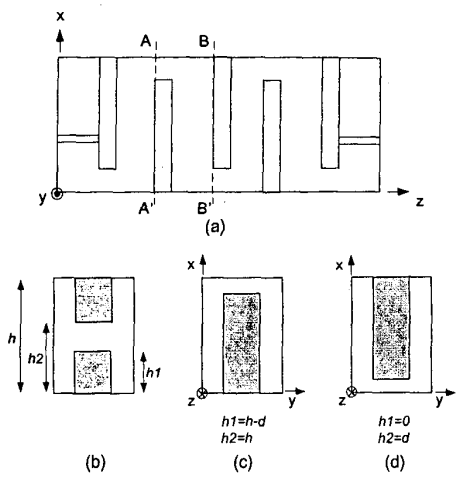

Fig. 5. (a) Top view of a general interdigital bandpass filter; cross sectional views of (b) general double-ridge waveguide bandpass filter, (c) plane AA' and (d) plane BB' of the interdigital filter showing the relationship in the analysis point of view.

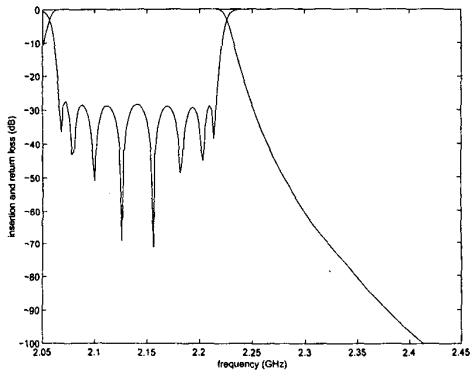

Fig. 7. Simulation results using mode matching for the filter configuration shown in Fig. 6.

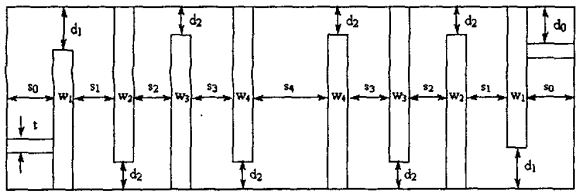

Dimensions (mil)		
d_0 : 210	s_0 : 390	w_1 : 129.17
d_1 : 65	s_1 : 234.90	w_2 : 227.12
d_2 : 78	s_2 : 257.86	w_3 : 224.58
t : 102.4	s_3 : 268.04	w_4 : 223.65
	s_4 : 270.33	

Fig. 6. Configuration and dimensions of the tapped-in interdigital 8 poles filter

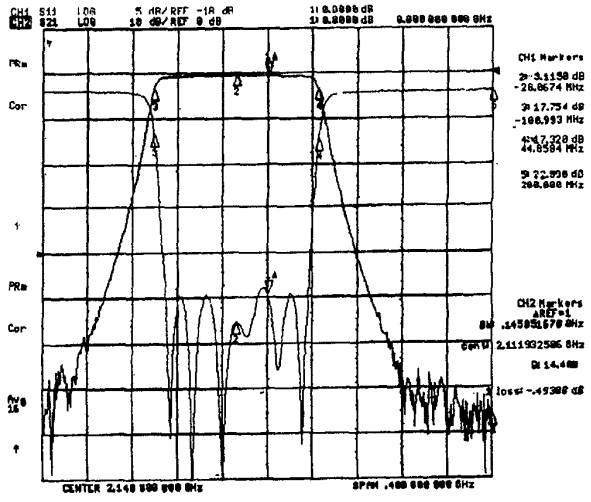

Fig. 8. Experimental results for the filter configuration shown in Fig. 6.